

Single-walled carbon nanotube growth from ion implanted Fe catalyst

Yongho Choi

Department of Electrical and Computer Engineering, University of Florida, Gainesville, Florida 32611

Jennifer Sippel-Oakley^{a)}

Department of Physics, University of Florida, Gainesville, Florida 32611

Ant Ural^{b)}

Department of Electrical and Computer Engineering, University of Florida, Gainesville, Florida 32611

(Received 14 May 2006; accepted 23 August 2006; published online 13 October 2006)

The authors present experimental evidence that single-walled carbon nanotubes can be grown by chemical vapor deposition from ion implanted iron catalyst. They systematically characterize the effect of ion implantation dose and energy on the catalyst nanoparticles and nanotubes formed at 900 °C. They also fabricate a micromachined silicon grid for direct transmission electron microscopy characterization of the as-grown nanotubes. This work opens up the possibility of controlling the origin of single-walled nanotubes at the nanometer scale and of integrating them into nonplanar three-dimensional device structures with precise dose control. © 2006 American Institute of Physics. [DOI: 10.1063/1.2360889]

Single-walled carbon nanotubes (SWCNTs), which have attracted a significant amount of research attention in recent years, are promising nanoscale materials as building blocks for electrical, mechanical, chemical, and biological devices and sensors. Nanotubes are generally produced by three main techniques: arc discharge, laser ablation, and chemical vapor deposition (CVD).¹

An essential component of the CVD growth process is the catalyst material placed on the substrate for nucleating the growth of carbon nanotubes. Typically, transition metal nanoparticles, such as nickel (Ni), iron (Fe), and cobalt (Co), are used as catalyst. For SWCNT growth, catalyst is usually spun on or dropdried from a liquid solution containing iron nanoparticles.² More recently, solid thin film layers deposited by evaporation or sputtering have also been used as catalyst.³ In order to control the origin of nanotubes during CVD growth, the catalyst is typically patterned by lithography into small “islands.”² However, it is not possible to pattern the liquid solution-based catalyst into very small dimensions or the thin film catalyst into nonplanar three-dimensional (3D) device structures, such as the sidewalls of high aspect ratio trenches. An alternative solution is to use ion implantation, a well-established technique in silicon microfabrication, and subsequent annealing to create catalyst nanoparticles. Ion implanted catalyst is much easier to pattern into very small features and over high aspect ratio topography compared to other types of catalyst, and it offers extremely accurate control of the number of atoms introduced into the substrate (the dose). Since ion implantation is very reproducible, easily scalable, and compatible with standard silicon microfabrication, it could offer significant technological advantages as a method to form catalyst nanoparticles.

A few previous experiments have shown that ion implantation and subsequent annealing can create catalyst nanoparticles for nucleating the growth of multiwalled carbon nanotubes (MWCNTs) having diameters of tens of nanometers.^{4–6} However, the growth of single-walled nanotubes from ion

implanted catalyst nanoparticles has not yet been demonstrated. In this letter, we present experimental evidence that single-walled carbon nanotubes can indeed be produced by the process of Fe ion implantation into thermally grown SiO₂ layers, subsequent annealing, and CVD growth. Furthermore, we systematically characterize the effect of implantation dose and energy on the structural properties of the catalyst nanoparticles and SWCNTs that are formed.

In our experiment, 500 nm thick SiO₂ layers were first thermally grown on silicon (100) substrates. Fe⁺ ions were implanted into these layers at an energy of 60 keV with three different doses (10¹⁴, 10¹⁵, and 10¹⁶ cm⁻²) and at a dose of 10¹⁵ cm⁻² with three different energies (25, 60, and 130 keV). The projected ranges R_p of the 25, 60, and 130 keV implants in SiO₂ are 23.9, 49.9, and 103.4 nm, respectively, based on SRIM (Ref. 7) calculations. The as-implanted samples were placed in a 1 in. quartz tube furnace and annealed at 900 °C under 300 sccm Ar and 200 sccm H₂ flow for 2 min to form the catalyst nanoparticles. After annealing, nanotubes were grown at the same temperature by discontinuing the Ar flow and introducing CH₄ at 200 sccm. The coflow of H₂ remained constant at 200 sccm, and the growth lasted for 10 min. The catalyst nanoparticles and nanotubes obtained were characterized by a Digital Instruments Nanoscope III atomic force microscope (AFM), a JEOL 2010F high resolution transmission electron microscope (HRTEM) operating at 100 kV, and a Renishaw Raman spectroscopy system.

The AFM images of Figs. 1(a)–1(c) show the Fe catalyst nanoparticles formed on the SiO₂ surface from implants of three different doses at 60 keV, after annealing the as-implanted substrates at 900 °C for 2 min. The average height and density of these nanoparticles are listed in Table I. It is clear from Fig. 1 that the low (10¹⁴ cm⁻²) implant dose results in very low density of catalyst particles, whereas the high (10¹⁶ cm⁻²) implant dose results in very large particle size. For the medium (10¹⁵ cm⁻²) dose sample, on the other hand, both small height (~2 nm) and high density Fe nanoparticles are obtained. Using a simple model, the flux of Fe atoms diffusing to the oxide surface is proportional to the

^{a)}Present address: IBM Microelectronics Division, Hopewell Junction, NY.

^{b)}Electronic mail: antural@ufl.edu

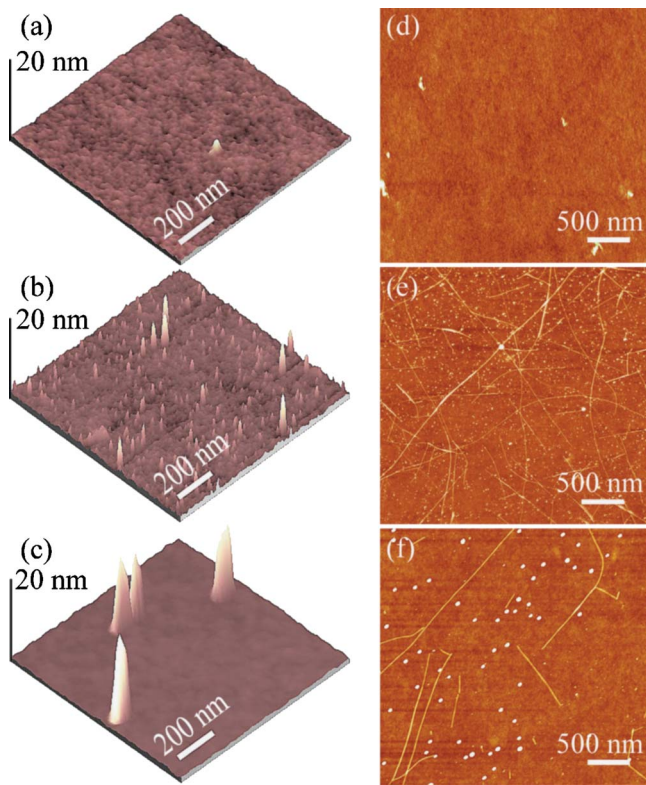


FIG. 1. (Color online) [(a)–(c)] AFM images of Fe catalyst nanoparticles formed after annealing the as-implanted SiO_2 substrates, and [(d)–(f)] Carbon nanotubes grown by CVD from the catalyst nanoparticles of (a)–(c), respectively. The Fe^+ implant doses are [(a) and (d)] 10^{14} , [(b) and (e)] 10^{15} , and [(c) and (f)] 10^{16} cm^{-2} at an energy of 60 keV.

dose of the implant; as a consequence, too little flux results in too few particles, and too much flux results in the aggregation of Fe atoms into larger clusters. Furthermore, we have also studied the effect of implant energy at a dose of 10^{15} cm^{-2} on the catalyst particle size and density, as presented in Table I. The low (25 keV) implant energy results in a very high density of catalyst particles with slightly larger average size than those obtained from the medium (60 keV) implant energy, whereas the high (130 keV) implant energy results in very large particle size and low density.

The AFM images of Figs. 1(d)–1(f) show the carbon nanotubes grown by CVD at 900°C from the catalyst nanoparticles shown in Figs. 1(a)–1(c), respectively. As seen in Fig. 1(d), no nanotubes were grown on the low dose sample, consistent with the very low density of catalyst nanoparticles

TABLE I. Average height and density of catalyst nanoparticles formed after annealing and the average diameter and density of nanotubes grown for each Fe ion implantation condition. Between 60–400 catalyst nanoparticles and 130–200 nanotubes from several different samples were characterized to obtain the values listed for each implantation condition.

Fe^+ ion implantation energy/dose (keV/ cm^{-2})	Catalyst nanoparticle height (nm)	Catalyst nanoparticle density (μm^{-2})	Nanotube diameter (nm)	Nanotube density (μm^{-2})
60/ 10^{14}	2.2	<1
60/ 10^{15}	2.0	170	2.2	6
60/ 10^{16}	15.0	4	2.2	1
25/ 10^{15}	2.7	800	2.8	7
130/ 10^{15}	21.0	6

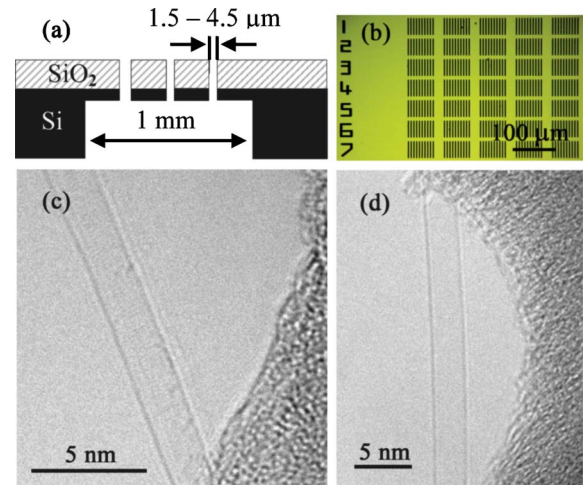


FIG. 2. (Color online) (a) Cross-sectional schematic (not to scale) and (b) top view optical microscope image of the micromachined Si TEM grids that we have fabricated. [(c) and (d)] HRTEM images obtained from the 60 keV, 10^{15} cm^{-2} Fe^+ implanted micromachined TEM grids, showing SWCNTs. All of the 85 nanotubes imaged by HRTEM were single-walled and no multi-walled nanotubes were observed.

on that sample. The high and medium dose samples, on the other hand, produced nanotubes with a similar average diameter (2.2 nm), although the density of nanotubes was much less for the high dose sample compared to the medium dose one (see Fig. 1 and Table I). This is due to the presence of a few small (~ 2 nm) catalyst nanoparticles on the high dose sample, despite the fact that the average catalyst size is much larger (15 nm). We have also studied the effect of implant energy at a dose of 10^{15} cm^{-2} on the nanotube diameter and density, as presented in Table I. The high implant energy did not produce any nanotubes due to the very large particle size, and the low implant energy resulted in nanotubes which have a slightly larger average diameter (~ 3 nm) than the medium energy sample, consistent with the slightly larger catalyst size.⁸ Table I shows that the nanotube yield is about four times higher for the 60 keV implant compared to the 25 keV implant at 10^{15} cm^{-2} dose. This could be due to two reasons: First, as previously observed, smaller Fe catalyst nanoparticles found in the 60 keV sample could be more active in producing SWCNTs compared to the larger ones found in the 25 keV sample.⁹ Second, during the 10 min growth step at 900°C , the implanted Fe atoms continue to outdiffuse towards the surface, and as a result, the density of catalyst nanoparticles continues to evolve. Based on AFM analysis, the densities of catalyst nanoparticles after growth for the 25 and 60 keV implants were found to be comparable. These experimental findings suggest that a lower implant energy does not necessarily result in a higher nanotube density.

In order to verify by HRTEM that the nanotubes grown from ion implanted catalyst are single-walled, we have fabricated special micromachined silicon substrates with narrow open slits on them, as shown in Figs. 2(a) and 2(b).¹⁰ Briefly, thin membranes of 1 mm^2 area were wet etched from the back side of a (100) Si wafer. Then, open slits of widths ranging from 1.5 to $4.5 \mu\text{m}$ and lengths of $50 \mu\text{m}$ were dry etched on these membranes from the top using a Si deep reactive ion etcher. Following the dry etch, a 300 nm thermal oxide was grown on the top surface, and the wafer was implanted with 60 keV, 10^{15} cm^{-2} Fe^+ ions. After dicing the wafer, the resulting Si substrates were annealed and CVD

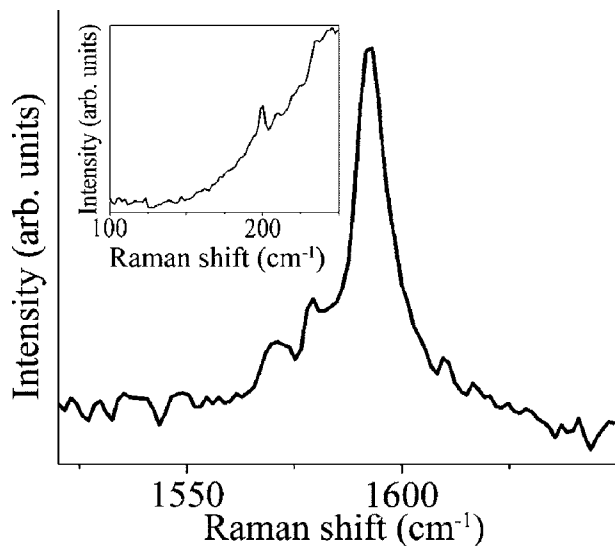


FIG. 3. Tangential mode (*G* band) micro-Raman spectra of nanotubes grown from 60 keV, 10^{15} cm $^{-2}$ Fe $^{+}$ implanted catalyst. A Lorentzian fit of the *G*-band spectrum yields peaks at 1570, 1579, and 1593 cm $^{-1}$. Inset shows radial breathing mode (RBM) Raman spectrum with a peak at 200 cm $^{-1}$, which corresponds to a SWCNT diameter of around 1.2 nm (Ref. 11).

grown, following the same procedure given above. The nanotubes grown on these substrates are completely suspended over the width of the slits, enabling direct TEM characterization of as-grown SWCNTs from ion implanted catalyst. The HRTEM images we have obtained show clear evidence that the as-grown nanotubes are single walled with diameters in agreement with the AFM data [see Figs. 2(c) and 2(d)]. The fact that MWCNTs and SWCNTs are not formed by the larger catalyst nanoparticles in our growth is due to the particular growth condition used, and this observation is consistent with previous work in the literature using similar growth conditions.^{8,9}

We have also characterized the nanotubes grown from the ion implanted catalyst (60 keV, 10^{15} cm $^{-2}$ Fe $^{+}$) using micro-Raman spectroscopy, as shown in Fig. 3. The Raman spectra were obtained by a Kr ion laser with an excitation wavelength of 647.1 nm and a spot size of about 1 μ m. The observation of characteristic multippeak tangential mode (*G* band) features around 1580 cm $^{-1}$ provides a signature of single-walled nanotubes.¹¹ A Lorentzian fit of the *G*-band spectrum in Fig. 3 yields peaks at 1570, 1579, and 1593 cm $^{-1}$. Furthermore, a radial breathing mode (RBM) peak at 200 cm $^{-1}$ is observed, as shown in the inset of Fig. 3, which corresponds to a SWCNT diameter of around 1.2 nm.¹¹ Since Raman experiments at a fixed laser energy

only detect nanotubes whose electronic energy spacings between van Hove singularities match the laser excitation energy, unlike AFM and HRTEM, Raman spectra do not give a complete characterization of the diameter distribution of nanotubes in a sample.¹¹ The nanotube diameter of 1.2 nm extracted from the RBM features shown in the inset of Fig. 3 falls within the diameter range of 0.8–3.5 nm observed by AFM and HRTEM. As a result, the Raman spectra also provide an independent confirmation of the existence of SWCNTs in our samples.

In conclusion, we have shown experimental evidence that single-walled carbon nanotubes can be grown by Fe ion implantation into SiO $_2$ /Si substrates, subsequent annealing, and CVD growth. For our growth condition, there is a dose and energy window in which nanotube growth is observed. In addition, we have fabricated a micromachined silicon grid for direct HRTEM characterization of CVD grown nanotubes, which can also be used to characterize other one-dimensional nanomaterials. This work opens up the possibility of controlling the origin of SWCNTs at the nanometer scale using advanced lithography techniques, such as electron-beam lithography, and of integrating nanotubes into nonplanar 3D device structures with precise dose control. Ion implantation could offer significant technological advantages as a method to form catalyst nanoparticles for a wide range of nanoscale device applications.

The authors would like to thank Andrew G. Rinzler for his help. This work was partially funded by Intel Corporation.

¹ *Carbon Nanotubes: Synthesis, Structure, Properties, and Applications*, edited by M. S. Dresselhaus, G. Dresselhaus, and P. Avouris (Springer, Berlin, 2001), Vol. 80, p. 30.

² J. Kong, H. T. Soh, A. M. Cassell, C. F. Quate, and H. Dai, *Nature* (London) **395**, 878 (1998).

³ L. Delzeit, B. Chen, A. Cassell, R. Stevens, C. Nguyen, and M. Meyyappan, *Chem. Phys. Lett.* **348**, 368 (2001).

⁴ J. M. Mao, L. F. Sun, L. X. Qian, Z. W. Pan, B. H. Chang, W. Y. Zhou, G. Wang, and S. S. Xie, *Appl. Phys. Lett.* **72**, 3297 (1998).

⁵ X. Z. Ding, L. Huang, X. T. Zeng, S. P. Lau, B. K. Tay, W. Y. Cheung, and S. P. Wong, *Carbon* **42**, 3030 (2004).

⁶ A. R. Adhikari, M. B. Huang, D. Wu, K. Dovidenko, B. Q. Wei, R. Vajtai, and P. M. Ajayan, *Appl. Phys. Lett.* **86**, 053104 (2005).

⁷ J. F. Ziegler and J. P. Biersack, www.srim.org

⁸ C. L. Cheung, A. Kurtz, H. Park, and C. M. Lieber, *J. Phys. Chem. B* **106**, 2429 (2002).

⁹ Y. Li, W. Kim, Y. Zhang, M. Rolandi, D. Wang, and H. Dai, *J. Phys. Chem. B* **105**, 11424 (2001).

¹⁰ Y. Choi, J. Johnson, R. Moreau, E. Perozziello, and A. Ural, *Nanotechnology* **17**, 4635 (2006).

¹¹ A. Jorio, M. A. Pimenta, A. G. Souza Filho, R. Saito, G. Dresselhaus, and M. S. Dresselhaus, *New J. Phys.* **5**, 139.1 (2003).